

Dark matter in the Galaxy

Neven Bilić[†], Gary B. Tupper, and Raoul D. Viollier[‡]

Institute of Theoretical Physics and Astrophysics,
Department of Physics, University of Cape Town,
Private Bag, Rondebosch 7701, South Africa

November 2, 2018

Abstract

After a brief introduction to standard cosmology and the dark matter problem in the Universe, we consider a self-gravitating noninteracting fermion gas at nonzero temperature as a model for the dark matter halo of the Galaxy. This fermion gas model is then shown to imply the existence of a supermassive compact dark object at the Galactic center.

1 Introduction

At some stage of the evolution of the Universe, primordial density fluctuations must have become gravitationally unstable forming dense clumps of dark matter (DM) that have survived until today in the form of galactic halos. In the recent past, galactic halos were successfully modeled as a self-gravitating isothermal gas of particles of arbitrary mass, the density of which scales asymptotically as r^{-2} , yielding flat rotation curves [1]. The aim of this paper is to describe the halo of our Galaxy in terms of a self-gravitating fermion gas in hydrostatic and thermal equilibrium at finite temperature.

Self-gravitating weakly interacting fermionic matter has been exploited in a wide range of astrophysical phenomena. Originally, self-gravitating degenerate neutrino stars were suggested as a model for quasars [2], and later neutrino matter was used as a model for dark matter in galactic halos and clusters of galaxies, with a neutrino mass in the \sim eV range [3]. Recently, degenerate superstars, composed of weakly interacting fermions in the \sim 10 keV range, were suggested [4, 5, 6, 7, 8] as an alternative to the supermassive black holes that are believed to exist at the centers of galaxies. It was shown [6] that such degenerate fermion stars could explain the whole range of supermassive compact dark objects which have been observed so far, with masses

[†]Permanent address: Rudjer Bošković Institute, P.O. Box 180, 10002 Zagreb, Croatia;
Email: bilic@thphys.irb.hr

[‡]Email: viollier@physci.uct.ac.za

ranging from 10^6 to $3 \times 10^9 M_\odot$, merely assuming that a weakly interacting quasistable fermion of mass $m \simeq 15$ keV exists in Nature. Most recently, it has been pointed out that a weakly interacting dark matter particle in the mass range $1 \lesssim m/\text{keV} \lesssim 5$ could solve the problem of the excessive structure generated on subgalactic scales in N -body and hydrodynamical simulations of structure formation in this Universe [9].

Of course, it is well known that the interval 1-15 keV lies squarely in the cosmologically forbidden mass range for stable active neutrinos ν [10]. The existence of such a massive active neutrino is also disfavored by the Super-Kamiokande data [11]. However, for an initial lepton asymmetry of $\sim 10^{-3}$, a sterile neutrino ν_s of mass $m_s \sim 10$ keV may be resonantly produced in the early Universe with near closure density, i.e., $\Omega \simeq 1$ [12]. The resulting energy spectrum is not thermal but rather cut off so that it approximates a degenerate Fermi gas. In this mass range, sterile neutrinos are also constrained by astrophysical bounds on the radiative $\nu_s \rightarrow \nu\gamma$ decay [13]. However, the allowed parameter space includes $m_s \simeq 15$ keV, contributing $\Omega_d \simeq 0.3$ to the critical density, as favored by the BOOMERANG data [14]. As an alternative possibility, the ~ 15 keV sterile neutrino could be replaced by the axino [15] or the gravitino [16, 17] in soft supersymmetry breaking scenarios.

As the supermassive compact dark objects at the galactic centers are well described by a degenerate gas of fermions, it is tempting to explore the possibility that one could describe both the supermassive compact dark objects and their galactic halos in a unified way in terms of a fermion gas at finite temperature. We will show that this is indeed the case, and that the observed dark matter distribution in the Galactic halo is consistent with the existence of a supermassive compact dark object at the center of the Galaxy which has about the right mass and size, and is in thermal and hydrostatic equilibrium with the halo.

2 Standard cosmology

Standard cosmology provides a successful description of the evolution of the Universe from a fraction of a second after the creation until today. A short review on the standard model of cosmology is given in [18]. For our purpose, it is sufficient to state the basic underlying principles. Standard cosmology is based on the following three theoretical assumptions:

1. Cosmological principle. The cosmological principle asserts that the Universe is homogeneous and isotropic on large scales. The most general metric satisfying the cosmological principle is the Friedmann-Robertson-Walker metric [19]

$$ds^2 = dt^2 - a(t)^2 \left[\frac{dr^2}{1 - kr^2} - r^2(d\theta^2 + \sin\theta d\phi^2) \right], \quad (1)$$

where the curvature constant k takes on the values 1, 0, or -1, for a closed, flat, or open universe, respectively. The time-dependent quantity $a(t)$ is the

scale factor of the expansion conveniently normalized to unity at present time, i.e., $a(t_0) = 1$. In other words, a is the radius of the Universe measured in units of its current radius.

2. General relativity. Gravity is described by Einstein's general theory of relativity governed by the *equivalence principle* and Einstein's field equations.

3. Perfect fluid. Matter is approximated by a homogeneous perfect fluid. The energy-momentum tensor then takes a simple form

$$T_{\mu\nu} = (\rho + p)u_\mu u_\nu - g_{\mu\nu}, \quad (2)$$

where ρ and p are the density and the pressure of the fluid, respectively.

With these assumptions, the set of Einstein's equations reduces to the Friedmann-Robertson-Walker (FRW) equations

$$H(t)^2 \equiv \left(\frac{\dot{a}}{a}\right)^2 = \frac{8\pi\rho}{3} - \frac{k}{a^2} + \frac{\Lambda}{3}, \quad (3)$$

$$\frac{\ddot{a}}{a} = \frac{\Lambda}{3} - 4\pi(\rho + 3p), \quad (4)$$

where the natural system of units $\hbar = c = G = 1$ is assumed. The first FRW equation describes the expansion of the Universe. The quantity $H(t)$ is the Hubble "constant" and Λ is the cosmological constant. We define the critical density as $\rho_{\text{cr}} = 3H_0^2/8\pi$ and the ratio of the density to the critical density is denoted by $\Omega = \rho/\rho_{\text{cr}}$. The precise present value of the Hubble constant is not known, but the widely accepted value is $H_0 = 100h_0 \text{ kms}^{-1}\text{Mpc}^{-1}$, with a dimensionless parameter h_0 between 0.4 and 1. Dividing by $H(t_0)^2$, Eq. (3) at $t = t_0$ can be conveniently written as a sum rule, i.e.,

$$\Omega_0 - k/(H_0 a_0)^2 + \Omega_\Lambda = 1, \quad (5)$$

where $\Omega_\Lambda = \Lambda/(3H_0^2)$ is the vacuum energy contribution to the critical density today. Observational evidence favors a flat universe today, i.e., $k = 0$. Thus, Eq. (5) becomes

$$\Omega_0 + \Omega_\Lambda = 1. \quad (6)$$

The second FRW equation (4) describes the acceleration of the expansion. The expansion will accelerate or decelerate, depending on whether the vacuum energy dominates the matter or vice versa. However, even if the cosmological term vanishes, the expansion could accelerate if the dominant component of the DM obeys a peculiar equation of state such that the pressure is negative and higher than one third of the density. One popular example is the scalar field model called *quintessence* [20]. Another scenario is based on a fluid obeying the Chaplygin gas equation of state $p \propto -1/\rho$ [21, 22], which has been intensively investigated for its solubility in 1+1-dimensional space-time, for its supersymmetric extension and connection to d -branes [23].

The observational evidence in support of standard cosmology may be summarized in four empirical pillars [24]: Hubble's law, cosmic background radiation (CBR), anisotropy of CBR, and abundance patterns of light elements. However, despite an overwhelming observational support, a number of problems remain unsolved:

- What caused the Big Bang and the expansion? Did the Universe begin with more than 3+1 dimensions?
- Why is the cosmological constant Λ about 50-120 orders of magnitude smaller than the value expected from quantum field theory?
- What caused the initial baryon-antibaryon asymmetry that led to the absence of antimatter today?
- Why is the Universe so smooth on large scales as evidenced by CBR?
- What caused the primordial density fluctuations that provided the seeds for structure formation?
- What does nonbaryonic DM consist of?

A solution to these problems most probably goes beyond the standard model of cosmology and certainly beyond the standard model of particle physics.

3 Dark matter

Here, we briefly discuss the DM problem and possible DM candidates. A more detailed analysis may be found in a number of recent review articles [25].

DM has to be introduced because of the following facts:

- Astronomical observations, such as the flatness of the rotation curves of spiral galaxies and the peculiar motion of galaxies within clusters, strongly indicate that

$$\Omega_0 \equiv \frac{\rho_{\text{matt}}}{\rho_{\text{cr}}} \gtrsim 0.3. \quad (7)$$

- Consistency with the Big Bang nucleosynthesis implies for baryonic matter

$$0.008h_0^{-2} < \Omega_B < 0.024h_0^{-2}. \quad (8)$$

- Astronomical observations yield a small relative density of luminous matter

$$\Omega_{\text{lum}} = 0.003h_0^{-1}. \quad (9)$$

From these facts we conclude that

- About 95% of matter is **dark**.
- About 60%-90% of DM is **nonbaryonic**.
- At least 75% of baryonic matter is **dark**.

Whereas baryonic DM is most likely in the form of relatively standard astrophysical objects, e.g., cold hydrogen clouds or compact objects such as neutron stars, brown dwarfs, MACHOs, and even black holes, the nature of nonbaryonic DM is unknown and still a subject of speculations. Candidates within the standard model are practically excluded and those beyond the standard model have not yet been detected in particle physics experiments. Nevertheless, cosmological and astrophysical observations tell us what these, yet undetected, particles could or could not be.

The different DM scenarios are conveniently classified as *hot*, *warm*, and *cold* DM [26], depending on the thermal velocities of DM particles in the early Universe.

Hot DM refers to low-mass neutral particles that are still relativistic when galaxy-size masses ($\sim 10^{12}M_\odot$) are first encompassed within the horizon. Hence, fluctuations on galaxy scales are wiped out by the “free streaming” of the dark matter. Standard examples of hot DM are neutrinos and majorons. They are still in thermal equilibrium after the QCD deconfinement transition, which took place at $T_{\text{QCD}} \simeq 150$ MeV. Hot DM particles have a cosmological number density comparable with that of microwave background photons, which implies an upper bound to their mass of a few tens of eV.

Warm DM particles are just becoming nonrelativistic when galaxy-size masses enter the horizon. Warm DM particles interact much more weakly than neutrinos. They decouple (i.e., their mean free path first exceeds the horizon size) at $T \gg T_{\text{QCD}}$. As a consequence, their number is expected to be roughly an order of magnitude lower and their mass an order of magnitude larger, than hot DM particles. Examples of warm DM are \sim keV sterile neutrinos, axinos [15], or gravitinos in soft supersymmetry breaking scenarios [16, 17]. There has been renewed interest in the standard model neutrino as a candidate for warm DM [27].

Cold DM particles are already nonrelativistic when even globular cluster masses ($\sim 10^6M_\odot$) enter the horizon. Hence, their free streaming is of no cosmological importance. In other words, all cosmologically relevant fluctuations survive in a universe dominated by cold DM. The two main particle candidates for cold dark matter are the lowest supersymmetric *weakly interacting massive particles* (WIMPs) and the *axion*.

One of the central issues in dark-matter modeling is the problem of structure formation on subgalactic scales. The combination of cold DM and a small cosmological constant (Λ CDM) seems to be in good agreement with many observational constraints. However, N-body and hydrodynamical simulations of galaxy formation evidence that Λ CDM overpredicts structure on small scales [9]. In addition to that, high-resolution simulations generally find a dark matter profile with a central cusp $\rho \propto r^{-1.5}$ for galactic halos [28, 29] which seems to contradict the observations.

Clustering on small scales could be suppressed by an upper limit to the phase-space density of DM particles owing either to degeneracy pressure if they are fermions or to a repulsive interaction if they are bosons. The fermion mass would have to lie in the range $0.1 \lesssim m \lesssim 10$ keV. A specific scenario invoking keV mass fermions is the *cool-dark-matter* proposal [13] for which

candidates exist in shadow-world models and the axino.

4 Galactic halo

We now discuss the properties of the halo of our Galaxy assuming that it consists of a self-gravitating gas of keV mass fermions in hydrostatic and thermal equilibrium at finite temperature. The Milky Way Galaxy consists of five major components which are nested within each other [30]. A spheroidal **halo** with modest concentrations of stars and about 170 globular clusters extends out to a radius of perhaps 200 kpc. Within a radius of ~ 25 kpc, the halo contains stars and open clusters that are concentrated into two essentially coplanar disks: the **thin disk** and the **thick disk**. In their innermost part the disks merge with a spheroidal **bulge**, the central concentration of luminous matter in the Galaxy. Finally, a compact dark object with a mass of $M_c \simeq 2.6 \times 10^6 M_\odot$ is located in the vicinity of the enigmatic radio source Sgr A* at the Galactic center [31], within a radius of 18 mpc.

Here, we demonstrate that by extending the Thomas-Fermi theory to nonzero temperature it is possible to explain, within the same model, both the Galactic halo and the compact dark object at the Galactic center. Extending the Thomas-Fermi theory to finite temperature [32, 33, 34], it has been shown that, at some critical temperature T_c , weakly interacting massive fermionic matter with a total mass below the Oppenheimer-Volkoff limit [35] undergoes a first-order gravitational phase transition from a diffuse to a clustered state, i.e., a nearly degenerate fermion star. However, during this first-order phase transition a large amount of latent heat must be released in order to substantially decrease the entropy of the initial diffuse configuration. In the absence of a mechanism which would make such a release possible, the system would remain in a thermodynamic quasistable supercooled state close to the point of gravothermal collapse. The Fermi gas will be caught in the supercooled state even if the total mass of the gas exceeds the Oppenheimer-Volkoff limit as a stable condensed state does not exist in this case.

The formation of a quasistable supercooled state may be understood as a process similar to that of violent relaxation, which was introduced to describe rapid virialization of stars of different mass in globular clusters [36, 37]. Through the gravitational collapse of an overdense fluctuation at about one Gyr after the Big Bang, part of gravitational energy transforms into the kinetic energy of random motion of small-scale density fluctuations. The resulting virialized cloud will thus be well approximated by a gravitationally stable thermalized halo. In order to estimate the mass-to-temperature ratio, we assume that an overdense cloud of mass M stops expanding at the time t_m , reaching its maximal radius R_m and the average density $\rho_m = 3M/(4\pi R_m^3)$. The total energy per particle is just the gravitational energy

$$E = -\frac{3}{5} \frac{M}{R_m}. \quad (10)$$

From the spherical model of nonlinear collapse [38] it follows

$$\rho_m = \frac{9\pi^2}{16}\bar{\rho}(t_m) = \frac{9\pi^2}{16}\Omega_d\rho_{\text{cr}}(1+z_m)^3, \quad (11)$$

where $\bar{\rho}(t_m)$ is the background density at the time t_m or the cosmological redshift z_m . We approximate the virialized cloud by a singular isothermal sphere [37] of the mass of the Galaxy M and radius R . The singular isothermal sphere is characterized by a constant circular velocity $\Theta = (2T/m)^{1/2}$ and the density profile

$$\rho(r) = \frac{\Theta^2}{4\pi r^2}. \quad (12)$$

Its total energy per particle is the sum of gravitational and thermal energies, i.e.,

$$E = -\frac{1}{4}\frac{M}{R} = -\frac{1}{4}\Theta^2. \quad (13)$$

Combining Eqs. (10), (11), and (13), we find

$$\Theta^2 = \frac{6\pi}{5}(6\Omega_d\rho_{\text{cr}}M^2)^{1/3}(1+z_m). \quad (14)$$

Taking $\Omega_d = 0.3$, $M = 2 \times 10^{12}M_\odot$, $z_m = 4$, and $h_0 = 0.65$, we find $\Theta \simeq 220 \text{ km s}^{-1}$, which corresponds to the mass-temperature ratio $m/T \simeq 4 \times 10^6$.

Next, we briefly discuss the general-relativistic Thomas-Fermi theory [34] for a self-gravitating gas, consisting of N fermions of mass m in equilibrium at a temperature T , enclosed in a sphere of radius R . We denote by p , ρ , and n the pressure, energy density, and particle number density of the gas, respectively. The metric generated by the mass distribution is static, spherically symmetric, and asymptotically flat, i.e.,

$$ds^2 = \xi^2 dt^2 - (1 - 2\mathcal{M}/r)^{-1} dr^2 - r^2(d\theta^2 + \sin\theta d\phi^2). \quad (15)$$

For numerical convenience, we introduce the parameter

$$\alpha = \frac{\mu}{T} \quad (16)$$

and the substitution

$$\xi = \frac{\mu}{m}(\varphi + 1)^{-1/2}, \quad (17)$$

where μ is the chemical potential associated with the conserved particle number N . Using this, the equation of state for a self-gravitating ideal gas may be represented in a parametric form [39]:

$$n = \frac{1}{\pi^2} \int_0^\infty dy \frac{y^2}{1 + \exp\{[(y^2 + 1)^{1/2}/(\varphi + 1)^{1/2} - 1]\alpha\}}, \quad (18)$$

$$\rho = \frac{1}{\pi^2} \int_0^\infty dy \frac{y^2(y^2 + 1)^{1/2}}{1 + \exp\{[(y^2 + 1)^{1/2}/(\varphi + 1)^{1/2} - 1]\alpha\}}, \quad (19)$$

$$p = \frac{1}{3\pi^2} \int_0^\infty dy \frac{y^4(y^2 + 1)^{-1/2}}{1 + \exp\{[(y^2 + 1)^{1/2}/(\varphi + 1)^{1/2} - 1]\alpha\}}. \quad (20)$$

We have chosen appropriate length and mass scales a and b , respectively, such that

$$a = b = \sqrt{\frac{2}{g}} \frac{1}{m^2}, \quad (21)$$

or, restoring \hbar , c , and G , we have

$$a = \sqrt{\frac{2}{g}} \frac{\hbar M_{\text{Pl}}}{cm^2} = 1.0798 \times 10^{10} \sqrt{\frac{2}{g}} \left(\frac{15\text{keV}}{m} \right)^2 \text{ km}, \quad (22)$$

$$b = \sqrt{\frac{2}{g}} \frac{M_{\text{Pl}}^3}{m^2} = 0.7251 \times 10^{10} \sqrt{\frac{2}{g}} \left(\frac{15\text{keV}}{m} \right)^2 M_{\odot}. \quad (23)$$

Here, $M_{\text{Pl}} = \sqrt{\hbar c/G}$ denotes the Planck mass and g the combined spin-degeneracy factor of neutral fermions and antifermions, i.e., $g=2$ or 4 for Majorana or Dirac fermions, respectively. In this way, the fermion mass, the degeneracy factor, and the chemical potential are eliminated from the equation of state.

Einstein's field equations for the metric (15) are given by

$$\frac{d\varphi}{dr} = -2(\varphi + 1) \frac{\mathcal{M} + 4\pi r^3 p}{r(r - 2\mathcal{M})}, \quad (24)$$

$$\frac{d\mathcal{M}}{dr} = 4\pi r^2 \rho. \quad (25)$$

To these two equations we add

$$\frac{d\mathcal{N}}{dr} = 4\pi r^2 (1 - 2\mathcal{M}/r)^{-1/2} n, \quad (26)$$

imposing the particle-number constraint as a condition at the boundary

$$\mathcal{N}(R) = N. \quad (27)$$

Equations (24)-(26) should be integrated using the boundary conditions at the origin:

$$\varphi(0) = \varphi_0 > -1; \quad \mathcal{M}(0) = 0; \quad \mathcal{N}(0) = 0. \quad (28)$$

It is useful to introduce the degeneracy parameter $\eta = \alpha\varphi/2$, which, in the Newtonian limit, approaches $\eta_{\text{nr}} = (\mu_{\text{nr}} - V)/T$. Here, we have introduced the nonrelativistic chemical potential $\mu_{\text{nr}} = \mu - m$, with $\mu_{\text{nr}} \ll m$, and the approximation $\xi = e^{V/m} \simeq 1 + V/m$, with V being the Newtonian potential. As φ is monotonously decreasing with increasing r , the strongest degeneracy is obtained at the center with $\eta_0 = \alpha\varphi_0/2$. The parameter η_0 , uniquely related to the central density and pressure, will eventually be fixed by the requirement (27). For $r \geq R$, the function φ yields the usual empty-space Schwarzschild solution

$$\varphi(r) = \frac{\mu^2}{m^2} \left(1 - \frac{2M}{r} \right)^{-1} - 1, \quad (29)$$

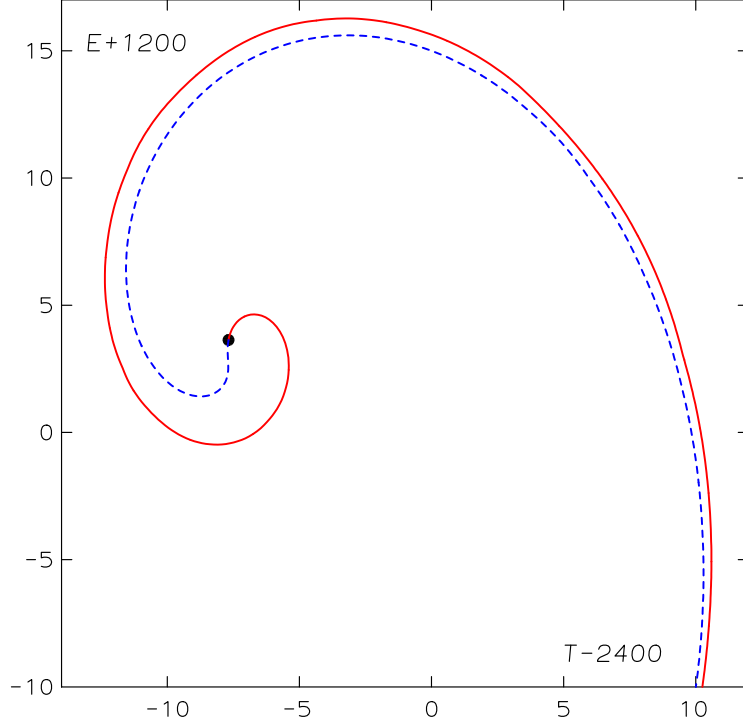


Figure 1: Energy (shifted by $12 \times 10^{-8}m$) versus temperature (shifted by $-24 \times 10^{-8}m$), both in units of $10^{-10}m$, for fixed $N = 2 \times 10^{12}M_{\odot}/m$

with

$$M = \mathcal{M}(R) = \int_0^R dr 4\pi r^2 \rho(r). \quad (30)$$

Given the temperature T , the set of self-consistency equations (18)-(26), with the boundary conditions (27)-(30) defines the general-relativistic Thomas-Fermi equation.

The numerical procedure is now straightforward. For a fixed, arbitrarily chosen α , we first integrate Eqs. (24) and (25) numerically on the interval $[0, R]$ and find solutions for various central values η_0 . Integrating (26) simultaneously, we obtain $\mathcal{N}(R)$ as a function of η_0 . We then select the value of η_0 for which $\mathcal{N}(R) = N$. The chemical potential μ corresponding to this particular solution is given by (29). If we now eliminate μ using (16), we finally get the parametric dependence on temperature through α .

The quantities N , T , and, R are free parameters in our model and their range and choice are dictated by physics. At $T = 0$ the number of fermions N is restricted by the OV limit $N_{\text{OV}} = 2.89 \times 10^9 \sqrt{2/g} (15 \text{ keV}/m)^2 M_{\odot}/m$.

However, at nonzero temperature, stable solutions exist with $N > N_{\text{OV}}$, depending on temperature and radius. In the following, N is required to be of the order $2 \times 10^{12} M_{\odot}/m$, so that for any m , the total mass is close to the estimated mass of the halo [40]. As we have demonstrated, the expected particle mass-temperature ratio of the halo is given by $\alpha \simeq m/T = 4 \times 10^4$. The halo radius R is in principle unlimited; in practice, however, it should not exceed half the average intergalactic distance. It is known that an isothermal configuration has no natural boundary, in contrast to the degenerate case of zero temperature, where for given N (up to the OV limit) the radius R is naturally fixed by the condition of vanishing pressure and density. At nonzero temperature, with R being unbounded, our gas would occupy the entire space, and fixing N would make p and ρ vanish everywhere. Conversely, if we do not fix N and integrate the equations on the interval $[0, \infty)$, both M and N will diverge at infinity for $T > 0$. Thus, one is forced to introduce a cutoff. In an isothermal model of a similar kind [41], the cutoff was set at the radius R , where the energy density was by about six orders of magnitude smaller than the central value. Our choice of $R = 200$ kpc is based on the estimated size of the Galactic halo.

The only remaining free parameters of our model are the fermion mass m and the degeneracy factor g , which always appear in the combination $m^4 g$. We fix these parameters at $m = 15$ keV and $g = 2$, and justify this choice *a posteriori*.

We now present the results of the calculations for fixed particle number and temperatures near the point of gravothermal collapse. In Fig. 1 the energy per particle defined as $E = M/N - m$ is plotted as a function of temperature for fixed $N = 2 \times 10^{12} M_{\odot}/m$. The plot looks very much like that of a canonical Maxwell-Boltzmann ensemble [37], with one important difference: in the Maxwell-Boltzmann case, the curve continues to spiral inwards *ad infinitum* approaching the point of the singular isothermal sphere, that is characterized by an infinite central density. In the Fermi-Dirac case, the spiral consists of two, almost identical curves. The inwards winding of the spiral begins for some negative central degeneracy and stops at the point $T = 2.3923 \times 10^{-7} m$, $E = -1.1964 \times 10^{-7} m$, where η_0 becomes zero. This part of the curve, which basically depicts the behavior of a nondegenerate gas, we call the *Maxwell-Boltzmann branch*. By increasing the central degeneracy parameter further to positive values, the spiral begins to unwind outwards very close to the inwards winding curve. The outwards winding curve will eventually depart from the Maxwell-Boltzmann branch for temperatures $T \gtrsim 10^{-3} m$. Further increase of the central degeneracy parameter brings us to a region where general-relativistic effects become important. The curve will exhibit another spiral for temperatures and energies of the order of a few $10^{-3} m$ approaching the limiting temperature $T_{\infty} = 2.4 \times 10^{-3} m$ and energy $E_{\infty} = 3.6 \times 10^{-3} m$, with both the central degeneracy parameter and the central density approaching infinite values. It is remarkable that gravitationally stable configurations with arbitrary large central degeneracy parameters exist at finite temperature even though the total mass exceeds the OV limit by several orders of magnitude.

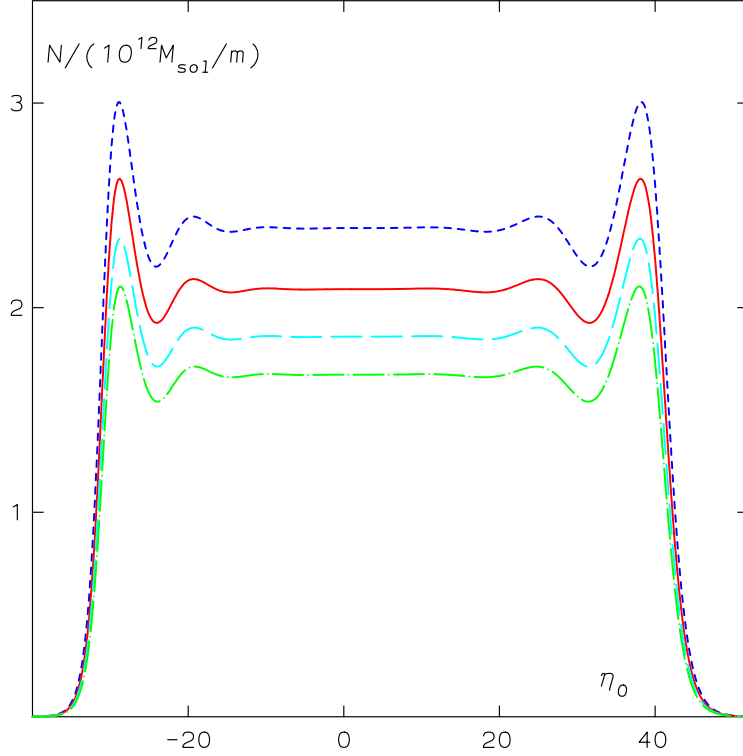


Figure 2: Number of particles versus central degeneracy parameter for $m/T = 4 \times 10^6$ (solid), 3.5×10^6 (short dashes), 4.5×10^6 (long dashes), and 5×10^6 (dot-dashed line).

The results of the numerical integration of Eqs. (24) and (25), without restricting N , are presented in Fig. 2, where we plot the particle number N as a function of the central degeneracy parameter η_0 for several values of α close to 4×10^6 . For fixed N , there is a range of α , where the Thomas-Fermi equation has multiple solutions. For example, for $N = 2 \times 10^{12}$ and $\alpha = 4 \times 10^6$ six solutions are found, which are denoted by (1), (2), (3), (3'), (2'), and (1'), corresponding to the values $\eta_0 = -30.528, -25.354, -22.390, 29.284, 33.380$, and 40.479 , respectively. In Figs. 3 and 4 we plot the corresponding density profiles and enclosed masses, respectively. For negative central value η_0 , for which the degeneracy parameter is negative everywhere, the system behaves basically as a Maxwell-Boltzmann isothermal sphere. Positive values of the central degeneracy parameter η_0 are characterized by a pronounced central core of mass of about $2.5 \times 10^6 M_\odot$ within a radius of about 20 mpc. The presence of this core is obviously due to the degeneracy pressure of the Fermi-Dirac statistics. A similar structure was obtained in

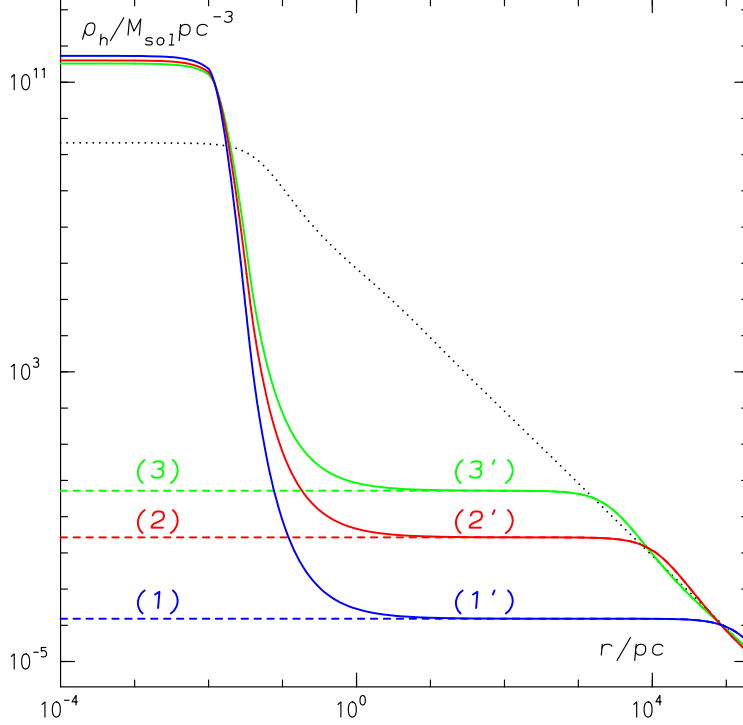


Figure 3: The density profile of the halo for a central degeneracy parameter $\eta_0 = 0$ (dotted line) and for the six η_0 -values discussed in the text. Configurations with negative η_0 ((1)-(3)) are depicted by the dashed and those with positive η_0 ((1')-(3')) by the solid line.

collisionless stellar systems modeled as a nonrelativistic Fermi gas [42].

Figs. 3 and 4 show two important features. First, a galactic halo at a given temperature T may or may not have a central core, depending on whether the central degeneracy parameter η_0 is positive or negative. As the potential is nearly harmonic up to about 1 to 10 kpc for negative η_0 , this may favor the formation of a barred galaxy. Second, the closer to zero η_0 is, the smaller the radius is at which the r^{-2} asymptotic behavior of the density begins. The flattening of the Galactic rotation curve begins in the range $1 \lesssim r/\text{kpc} \lesssim 10$, hence the solution (3') most likely describes the Galaxy's halo. This may be verified by calculating the rotational curves in our model. We know already from our estimate (14) that our model yields the correct asymptotic circular velocity of 220 km/s. In order to make a more realistic comparison with the observed Galactic rotation curve, we must include two additional matter components: the bulge and the disk. The bulge is modeled as a spherically

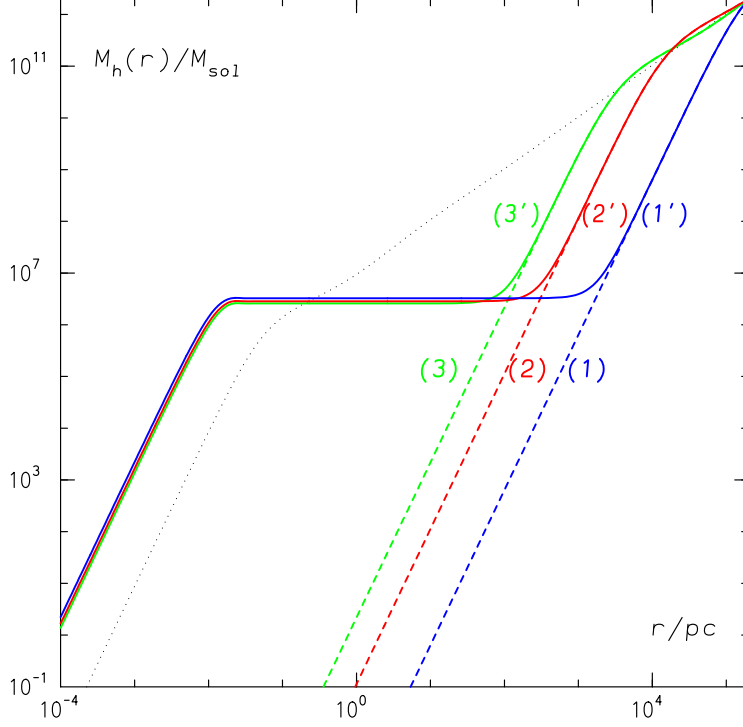


Figure 4: Mass of the halo $M_h(r)$ enclosed within a radius r for various central degeneracy parameters η_0 as in Fig. 3.

symmetric matter distribution of the form [43]

$$\rho_b(s) = \frac{e^{-hs}}{2s^3} \int_0^\infty du \frac{e^{-hsu}}{[(u+1)^8 - 1]^{1/2}}, \quad (31)$$

where $s = (r/r_0)^{1/4}$, r_0 is the effective radius of the bulge and h is a parameter. We adopt $r_0 = 2.67$ kpc and h yielding the bulge mass $M_b = 1.5 \times 10^{10} M_\odot$ [44]. In Fig. 5 the mass of halo and bulge enclosed within a given radius is plotted for various η_0 . Here, the gravitational backreaction of the bulge on the fermionic halo has been taken into account. The data points, indicated by squares, are the mass $M_c = 2.6 \times 10^6 M_\odot$ within 18 mpc, estimated from the motion of the stars near Sgr A* [45], and the mass $M_{50} = 5.4_{-3.6}^{+0.2} \times 10^{11}$ within 50 kpc, estimated from the motions of satellite galaxies and globular clusters [40]. Variation of the central degeneracy parameter η_0 between 24 and 32 does not change the essential halo features.

In Fig. 6 we plot the circular velocity components of the halo, the bulge,

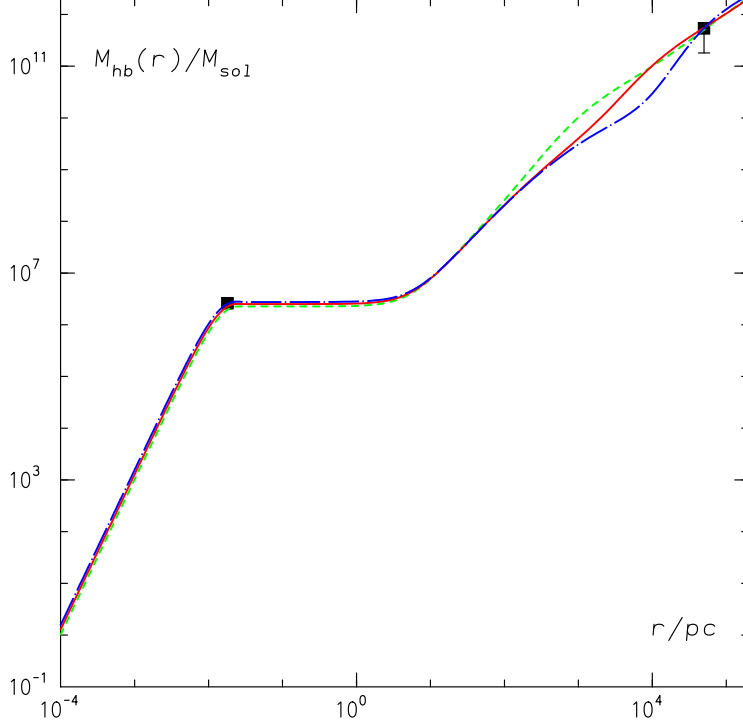


Figure 5: Enclosed mass of halo plus bulge versus radius for $\eta_0 = 24$ (dashed), 28 (solid), and 32 (dot-dashed line).

and the disk. The contribution of the disk is modeled as [46]

$$\Theta_d(r)^2 = \Theta_d(r_o)^2 \frac{1.97(r/r_o)^{1.22}}{[(r/r_o)^2 + 0.78^2]^{1.43}}, \quad (32)$$

where we have taken $r_o = 13.5$ kpc and $\Theta_d = 100$ km/s. Here it is assumed for simplicity that the disk does not influence the mass distribution of the bulge and the halo. Choosing the central degeneracy $\eta_0 = 28$ for the halo, the data by Merrifield and Olling [47] are reasonably well fitted.

We now turn to the discussion of our choice of the fermion mass $m = 15$ keV for the degeneracy factor $g = 2$. To that end, we investigate how the mass of the central object, i.e., the mass M_c within 18 mpc, depends on m in the interval 5 to 25 keV, for various η_0 . We find that $m \simeq 15$ keV always gives the maximal value of M_c ranging between 1.7 and $2.3 \times 10^6 M_\odot$ for η_0 between 20 and 28. Hence, with $m \simeq 15$ keV we get the value closest to the mass of the central object M_c estimated from the motion of the stars near Sgr A* [45].

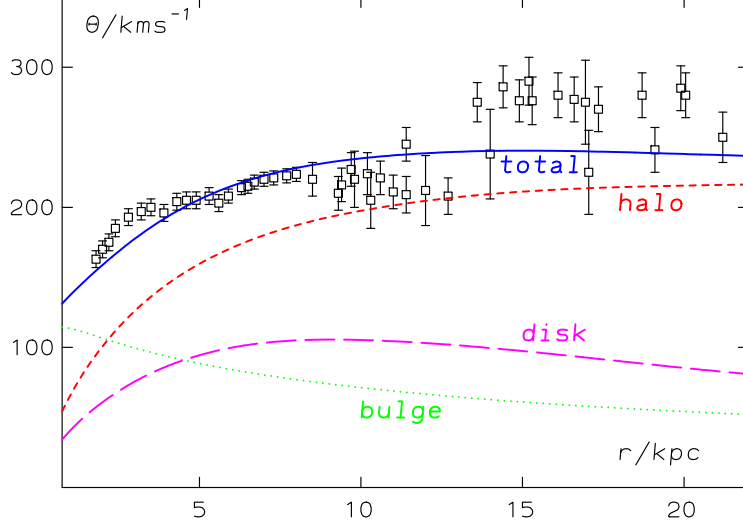


Figure 6: Fit to the rotation curve of the Galaxy. The data points are from [47] for $R_0 = 8.5$ kpc and $\Theta_0 = 220$ km/s.

5 Conclusions

In summary, using the Thomas-Fermi theory, we have shown that a weakly interacting fermionic gas at finite temperature yields a mass distribution that successfully describes both the center and the halo of the Galaxy. For a fermion mass $m \simeq 15$ keV, a reasonable fit to the rotation curve is achieved with the temperature $T = 3.75$ meV and the central degeneracy parameter $\eta_0 = 28$. With the same parameters, we obtain the mass $M_{50} = 5.04 \times 10^{11} M_\odot$ and $M_{200} = 2.04 \times 10^{12} M_\odot$ within 50 and 200 kpc, respectively. These values agree quite well with the mass estimates based on the motions of satellite galaxies and globular clusters [40]. Moreover, the mass of $M_c \simeq 2.27 \times 10^6 M_\odot$, enclosed within 18 mpc, agrees reasonably well with the observations of motion of stars near the compact dark object at the center of the Galaxy.

Acknowledgement

We thank P. Salucci for valuable discussions and comments. We are grateful to M.R. Merrifield and R.P. Olling for sending us the Galactic rotation curve. This research is in part supported by the Foundation of Fundamental Research (FFR) grant number PHY99-01241 and the Research Committee of the University of Cape Town. The work of N.B. is supported in part by the Ministry of Science and Technology of the Republic of Croatia under Contract No. 0098002.

References

- [1] S. Cole and C. Lacey, Mon. Not. R. Astron. Soc. **281**, 716 (1996), and references therein.
- [2] M.A. Markov, Phys. Lett. **10**, 122 (1964).
- [3] G. Marx and A.S. Szalay, in *Neutrino '72*, **1**, 191 (Technoinform, Budapest, 1972); R. Cowsik and J. McClelland, Astrophys. J. **180**, 7 (1973); R. Ruffini, Lett. Nuovo Cim. **29**, 161 (1980).
- [4] R.D. Viollier, D. Trautmann, and G.B. Tupper, Phys. Lett. B **306**, 79 (1993); R.D. Viollier, Prog. Part. Nucl. Phys. **32**, 51 (1994).
- [5] N. Bilić, D. Tsiklauri, and R.D. Viollier, Prog. Part. Nucl. Phys. **40**, 17 (1998); N. Bilić and R.D. Viollier, Nucl. Phys. (Proc. Suppl.) B **66**, 256 (1998).
- [6] N. Bilić, F. Munyaneza, and R.D. Viollier, Phys. Rev. D **59**, 024003 (1999).
- [7] D. Tsiklauri, and R.D. Viollier, Astropart. Phys. **12**, 199 (1999); F. Munyaneza and R.D. Viollier, astro-ph/9907318.
- [8] F. Munyaneza, D. Tsiklauri, and R.D. Viollier, Astrophys. J. **509**, L105 (1998); *ibid.* **526**, 744 (1999); F. Munyaneza and R.D. Viollier, astro-ph/0103466, Astrophys. J. **563**, 0000 (2001).
- [9] P. Bode, J.P. Ostriker, and N. Turok, Astrophys. J. **556**, 93 (2001), astro-ph/0010389.
- [10] E.W. Kolb and M.S. Turner, *The Early Universe*, (Addison-Wesley, San Francisco, 1989).
- [11] S. Fukuda *et al.*, Phys. Rev. Lett. **85**, 3999 (2000).
- [12] X. Shi and G.M. Fuller, Phys. Rev. Lett. **82**, 2832 (1999); K. Abazajian, G.M. Fuller, and M. Patel, Phys. Rev. D **64**, 023501 (2001), astro-ph/0101524; G.B. Tupper, R.J. Lindebaum, and R.D. Viollier, Mod. Phys. Lett. A **15**, 1221 (2000).

- [13] M. Drees and D. Wright, hep-ph/0006274.
- [14] P. de Bernardis *et al.*, Nature **404**, 955 (2000).
- [15] T. Goto and M. Yamaguchi, Phys. Lett. B **276**, 123 (1992); L. Covi , J.E. Kim, and L. Roszkowski, Phys. Rev. Lett. **82**, 4180 (1999), hep-ph/9905212; L. Covi , H.-B. Kim, J.E. Kim, and L. Roszkowski, hep-ph/0101009.
- [16] M. Dine and A.E. Nelson, Phys. Rev. D **48**, 1277 (1993), hep-ph/9303230; M. Dine, A.E. Nelson, and Y. Shirman, Phys. Rev. D **51**, 1362 (1995), hep-ph/9408384; M. Dine, A.E. Nelson, Y. Nir, and Y. Shirman, Phys. Rev. D **53**, 2658 (1996), hep-ph/9507378; D.H. Lyth, Phys. Lett. B **488**, 417 (2000), hep-ph/9911257.
- [17] H. Murayama, Phys. Rev. Lett. **79**, 18 (1997), hep-ph/9705271; S. Dimopoulos, G. Dvali, R. Rattazzi, and G.F. Giudice, Nucl. Phys. B **510**, 12 (1998), hep-ph/9705307; E.A. Baltz and H. Murayama, astro-ph/0108172.
- [18] E.W. Kolb and M.S. Turner, in *Review of Particle Physics*, Eur. Phys. J. C **15**, 1 (2000).
- [19] S. Weinberg, “Gravitation and Cosmology” (Wiley, New York, 1972).
- [20] C. Wetterich, Nucl. Phys. B **302**, 668 (1988); P.J.E. Peebles and B. Ratra, Astrophys. J. **325**, L17 (1988); R. Caldwell, R. Dave, and P.J. Steinhardt, Phys. Rev. Lett. **80**, 1589 (1998); D. Huterer and M.S. Turner, Phys. Rev. D **60**, 081301 (1999).
- [21] A. Kamenshchik, U. Moschella, and V. Pasquier, Phys. Lett. B **511**, 265 (2001).
- [22] N. Bilić, G.B. Tupper, and R.D. Viollier, astro-ph/0111325.
- [23] Y. Bergner and R. Jackiw, Phys. Lett. A **284**, 146 (2001); for a review see R. Jackiw, physics/0010042.
- [24] M.S. Turner, Phys. World **9**, No 9, 31 (1996).
- [25] A.D. Dolgov, hep-ph/9910532; M. Srednicki, in *Review of Particle Physics*, Eur. Phys. J. C **15**, 1 (2000); L. Bergstrom, Rep. Prog. Phys. **63**, 793 (2000), hep-ph/0002126.
- [26] J.R. Primack, in *Formation of Structure in the Universe*, eds. A. Dekel and J.P. Ostriker (Cambridge University Press, 1999), astro-ph/9707285.
- [27] G.F. Giudice, E.W. Kolb, A. Riotto, D.V. Semikoz, and I. Tkachev, Phys. Rev. D **64**, 043512 (2001), hep-ph/0012317.
- [28] A. Klypin et al., Astrophys. J. **554**, 903 (2001).

- [29] B. Moore et al., Phys. Rev. D in press, astro-ph/0106217.
- [30] R. Buser, Science **287**, 69 (2000).
- [31] R. Mahadevan, Nature **394**, 651 (1998).
- [32] W. Thirring, Z. Physik **235**, 339 (1970); P. Hertel, H. Narnhofer, and W. Thirring, Comm. Math. Phys. **28**, 159 (1972); J. Messer, J. Math. Phys. **22**, 2910 (1981).
- [33] N. Bilić and R.D. Viollier, Phys. Lett. B **408**, 75 (1997).
- [34] N. Bilić and R.D. Viollier, Gen. Rel. Grav. **31**, 1105 (1999); Eur. Phys. J. C **11**, 173 (1999).
- [35] J.R. Oppenheimer and G.M. Volkoff, Phys. Rev. **55**, 374 (1939).
- [36] D. Lynden-Bell, Mon. Not. R. Astron. Soc. **136**, 101 (1967).
- [37] J. Binney and S. Tremaine, *Galactic Dynamics* (Princeton University Press, Princeton, New Jersey, 1987), and references cited therein.
- [38] T. Padmanabhan, *Structure formation in the Universe* (Cambridge University Press, Cambridge, 1993).
- [39] J. Ehlers, in *Relativity, Astrophysics and Cosmology*, edited by W. Israel (D. Reidel Publishing Company, Dordrecht/Boston 1973)
- [40] M.I. Wilkinson and N.W. Evans, Mon. Not. R. Astron. Soc. **310**, 645 (1999).
- [41] W.Y. Chau, K. Lake, and J. Stone, Astrophys. J. **281**, 560 (1984).
- [42] P.-H. Chavanis and J. Sommeria, Mon. Not. R. Astron. Soc. **296**, 569 (1998).
- [43] P.J. Young, Astrophys. J. **81**, 807 (1976); G. de Vaucouleurs and W.D. Pence, Astrophys. J. **83**, 1163 (1978).
- [44] P.D. Sackett, Astrophys. J. **483**, 103 (1997).
- [45] A. Eckart and R. Genzel, Mon. Not. R. Astron. Soc. **284**, 576 (1997); A.M. Ghez, B.L. Klein, M. Morris, and E.E. Becklin, Astrophys. J. **509**, 678 (1998).
- [46] M. Persic, P. Salucci, and F. Stell, Mon. Not. R. Astron. Soc. **281**, 27 (1986).
- [47] R.P. Olling and M.R. Merrifield, Mon. Not. R. Astron. Soc. **311**, 361 (2000).